

MMP-9 Responsive PEG Cleavable Nanovesicles for Efficient Delivery of Chemotherapeutics to Pancreatic Cancer

Prajakta S. Kulkarni,[†] Manas K. Haldar,[†] Rahul R. Nahire,[†] Preeya Katti,[‡] Avinash H. Ambre,[§] Wallace W. Muhonen,^{||} John B. Shabb,^{||} Sathish K. R. Padi,[†] Raushan K. Singh,[⊥] Pawel P. Borowicz,[#] D. K. Shrivastava,[⊥] Kalpana S. Katti,[§] Katie Reindl,[¶] Bin Guo,[†] and Sanku Mallik^{*,†}

[†]Department of Pharmaceutical Sciences, North Dakota State University, Fargo, North Dakota 58102, United States

[‡]Davies High School, Fargo, North Dakota 58104, United States

[§]Department of Civil and Environmental Engineering, North Dakota State University, Fargo, North Dakota 58102, United States

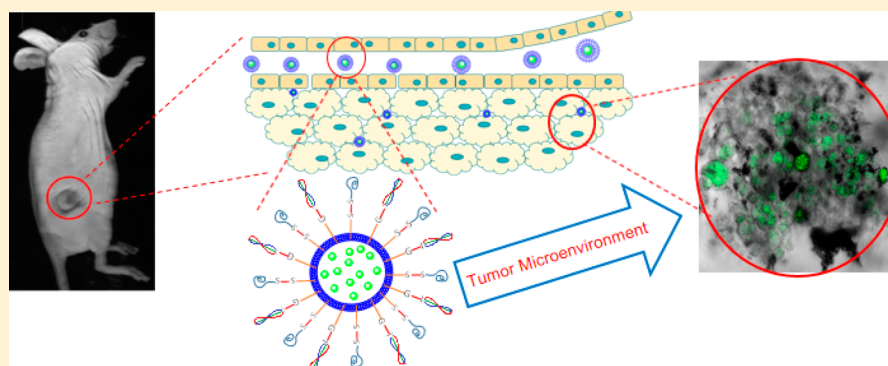
^{||}Department of Biochemistry, University of North Dakota, Grand Forks, North Dakota 58202, United States

[⊥]Department of Chemistry and Biochemistry, North Dakota State University, Fargo, North Dakota 58102, United States

[#]Department of Animal Sciences, North Dakota State University, Fargo, North Dakota 58102, United States

[¶]Department of Biological Sciences, North Dakota State University, Fargo, North Dakota 58102, United States

Supporting Information



ABSTRACT: Significant differences in biochemical parameters between normal and tumor tissues offer an opportunity to chemically design drug carriers which respond to these changes and deliver the drugs at the desired site. For example, overexpression of the matrix metalloproteinase-9 (MMP-9) enzyme in the extracellular matrix of tumor tissues can act as a trigger to chemically modulate the drug delivery from the carriers. In this study, we have synthesized an MMP-9-cleavable, collagen mimetic lipopeptide which forms nanosized vesicles with the POPC, POPE-SS-PEG, and cholesteryl-hemisuccinate lipids. The lipopeptide retains the triple-helical conformation when incorporated into these nanovesicles. The PEG groups shield the substrate lipopeptides from hydrolysis by MMP-9. However, in the presence of elevated glutathione levels, the PEG groups are reductively removed, exposing the lipopeptides to MMP-9. The resultant peptide-bond cleavage disturbs the vesicles' lipid bilayer, leading to the release of encapsulated contents. These PEGylated nanovesicles are capable of encapsulating the anticancer drug gemcitabine with 50% efficiency. They were stable in physiological conditions and in human serum. Effective drug release was demonstrated using the pancreatic ductal carcinoma cells (PANC-1 and MIAPaCa-2) in two-dimensional and three-dimensional "tumor-like" spheroid cultures. A reduction in tumor growth was observed after intravenous administration of the gemcitabine-encapsulated nanovesicles in the xenograft model of athymic, female nude mice.

KEYWORDS: drug delivery, drug release, matrix metalloproteinase-9, peptide, nanoparticle, pancreatic cancer cell spheroids

1. INTRODUCTION

Stimulus-responsive nanomaterials deliver encapsulated drugs preferentially at the target site, enhancing the therapeutic benefits and minimizing drug-related cytotoxicity.¹ Several extraneous sources of energy, such as temperature, light, magnetic field, ultrasound, etc., have been used to release the encapsulated drugs from the nanomaterials.² Internal stimulus-responsive carriers use the inherent biochemical differences

between physiological and cancerous tissues when delivering the drugs to the affected site.³ Because several enzymes are overexpressed in the cancerous tissues, the enzymes have been

Received: February 5, 2014

Revised: April 15, 2014

Accepted: May 14, 2014

Published: May 14, 2014

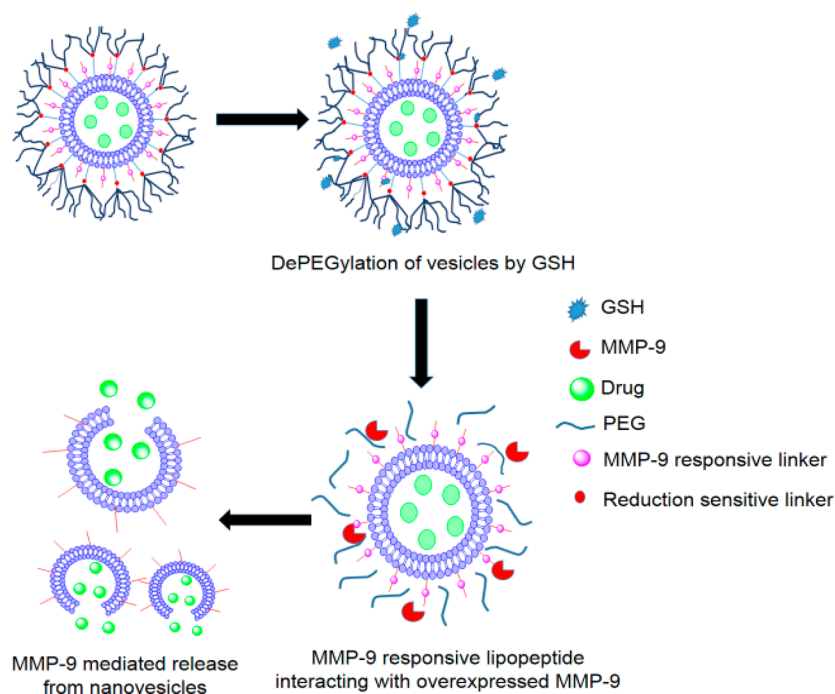
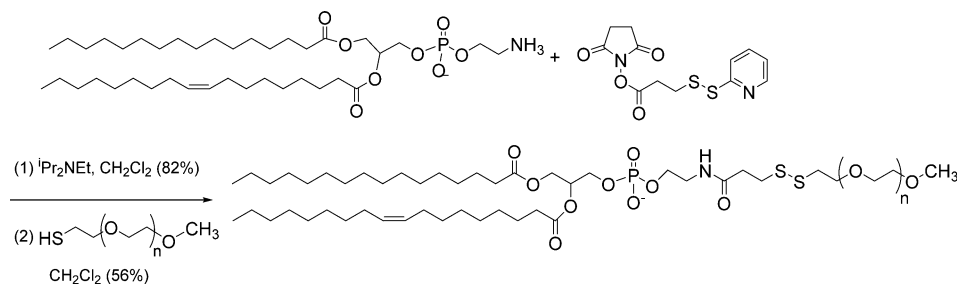


Figure 1. Schematic representation of nanovesicles incorporating MMP-9 substrate lipopeptides and reduction-sensitive POPE-SS-PEG which render the nanovesicles responsive to extracellular, elevated levels of MMP-9 and GSH.

Scheme 1. Synthetic Scheme for POPE-SS-PEG



used as triggers to release the contents from appropriate carriers.⁴

The extracellular matrix metalloproteinase (MMP) proteolytic enzymes are overexpressed in many types of tumors and play a crucial role in cancer invasion and metastasis.⁵ MMP-2 and MMP-9 have been investigated as triggers by employing enzyme-responsive peptides on the surface of the carriers.⁶ However, in a dynamic physiological environment, the drug carrier needs to be stable before it reaches the tumor site. Coating the nanoparticles with poly(ethylene glycol) polymer (PEGylation) reduces the unintended interactions with circulating proteins.⁷ This PEG coating reduces the interfacial tension and hinders protein adsorption on the nanoparticles' surface.⁸ Hence, PEGylated nanoparticles accumulate at the tumor site due to the enhanced permeation and retention (EPR) effect.⁹ However, at the tumor site, the PEG layer needs to be removed from the carriers to elicit the desired effects.¹⁰

Matrix metalloproteinase levels are often elevated in the extracellular matrix of various cancers, including pancreatic cancer.¹¹ In the present study, we have synthesized an MMP-9-cleavable, collagen mimetic lipopeptide which formed nano-sized vesicles with 1-palmitoyl-2-oleoyl-*sn*-glycero-3-phosphocholine (POPC), cholesteryl-hemisuccinate, and the synthesized reduction sensitive, PEGylated 1-palmitoyl-2-oleoyl-*sn*-

glycero-3-phosphoethanolamine lipid (POPE-SS-PEG₅₀₀₀). The PEG₅₀₀₀ in POPE-SS-PEG₅₀₀₀ was incorporated to render long circulating characteristic to nanovesicles. In the extracellular matrix of the tumors, we anticipated that the POPE-SS-PEG₅₀₀₀ polymer would undergo reduction by glutathione and shed the PEG chains. The de-PEGylation from the surface of nanovesicles will expose the MMP-9-responsive, collagen mimetic lipopeptides to enzymatic hydrolysis. The resultant destabilization of the nanovesicles will trigger the release of the encapsulated drugs (Figure 1). We note that, besides MMP-9, the increased levels of extracellular MMP-2 and intracellular glutathione (GSH) in tumors have been used to shed PEG from the surface of the drug carrier for *in vitro* studies.^{8,9,12–15}

We validated and optimized this delivery strategy by monitoring the release profiles of the encapsulated dye carboxyfluorescein in the presence of physiologically relevant concentrations of GSH and MMP-9. Subsequently, the anticancer drug gemcitabine was encapsulated in the optimized nanovesicles, and cytotoxicity was determined by employing two-dimensional monolayer cultures of human pancreatic cancer cells. However, we note that the conventional monolayer cultures of cancer cells lack the three-dimensional, cell–cell interactions that are encountered with the *in vivo* environments.¹⁶ Three-dimensional, spheroid cell cultures have

been proposed to bridge this gap between conventional monolayer cultures and animal-model studies.¹⁷ The human pancreatic cancer cell line PANC-1 forms such spheroids which can provide the three-dimensional architecture encountered by drug carriers *in vivo*.¹⁸ In this study, we tested the cytotoxicity of gemcitabine-encapsulated nanovesicles in PANC-1 cell spheroids and also in a mouse xenograft model.

2. MATERIALS AND METHODS

The POPE-S-S-PEG disulfide lipid was synthesized as shown in Scheme 1. Synthetic details for this lipid, as well as for the LP lipopeptide, are provided in the Supporting Information.

2.1. Preparation of Carboxyfluorescein Encapsulated Nanovesicles. The nanovesicles (liposomes) were prepared by mixing POPC lipid (Avanti Polar Lipids), synthesized lipopeptide LP, POPE-SS-PEG₅₀₀₀, and cholesteryl hemisuccinate in molar proportions of 60:30:5:5, respectively. All the lipids were dissolved in chloroform. The chloroform was removed using a rotary evaporator to form a thin lipid film in a round-bottom flask. The film was further vacuum-dried overnight inside a desiccator. The film was then hydrated at 60 °C for 2 h with 100 mM carboxyfluorescein solution prepared in HEPES buffer (pH 7.4). The formed vesicles were subjected to ultrasonication for 45 min using an Aquasonic bath sonicator (model 250D, power level 9). The resulting vesicles were then extruded through 0.8 μm and, subsequently, 0.2 μm filters to obtain vesicles with a uniform size. To remove the unencapsulated dye, the vesicles were passed through a Sephadex G50-size exclusion column, and an orange band of carboxyfluorescein-encapsulated nanovesicles was collected. These vesicles were used for the release and imaging experiments. Since a large excess of carboxyfluorescein was used, we did not estimate the percentage of the dye encapsulated.

2.2. Preparation of Gemcitabine-Encapsulated Nanovesicles. Gemcitabine was encapsulated in the nanovesicles with the pH gradient method.¹⁹ Nanovesicles of lipid composition POPC (Avanti Polar Lipids), LP, POPE-SS-PEG, cholesteryl hemisuccinate, and lissamine rhodamine lipid (Avanti Polar Lipids) were prepared by dissolving them in chloroform in the molar proportions of 59:30:5:5:1, respectively. Chloroform was then evaporated under reduced pressure, and the resulting thin film of lipids was dried under a vacuum desiccator. This film was hydrated with 2 mL of 20 mM citric acid buffer (pH 4). The resulting vesicles were subjected to ultrasonication for 45 min (at power level 9) and were then extruded through a 0.2 μm filter. Nanovesicles were collected after being passed through a Sephadex G50 gel-filtration column. Lissamine rhodamine lipid (1 mol %) was incorporated in these nanovesicles to impart color, and to aid in visualizing the vesicles during size exclusion chromatography. These eluted nanovesicles (pH 7.4) were incubated with 1 mg/mL aqueous solution of gemcitabine at 60 °C for 2 h. The gemcitabine solution was added to the nanovesicles to create a lipid–drug ratio of 10:1. Drug-carrying nanovesicles were again passed through the Sephadex G50 column to remove nonencapsulated gemcitabine. Entrapment efficiency of the nanovesicle was then calculated to be 50% (Supporting Information). These nanovesicles were used for cytotoxicity studies.

2.3. Size and Morphology Analysis. The hydrodynamic diameters of the vesicles were measured using a dynamic light scattering (DLS) instrument (Malvern Zetasizer Nano-ZS90).

Measurements were conducted at a scattering angle of 90° using a polystyrene, latex disposable cuvette. An equilibration time of 120 s was kept constant for all measurements. For each sample, 6 readings were recorded averaging 6 runs for the same sample. In order to observe size changes in the presence of added MMP-9 and GSH, the nanovesicles that encapsulated gemcitabine were incubated with MMP-9 and GSH. Size changes were monitored for 24 h with DLS, and the morphology change was observed using an atomic force microscope (AFM). For AFM imaging, the nanovesicles were deposited on a mica sheet and were imaged using a MultiMode atomic force microscope with a Nanoscope IIIa controller and a J-type piezo scanner (Veeco Metrology Group, Santa Barbara, CA). An antimony (n) doped Si tip was used for obtaining images in the tapping mode.

2.4. Release Studies. The release of the encapsulated dye was monitored with a fluorescence spectrofluorometer (Spectramax-M5, Molecular Devices, Inc.). Carboxyfluorescein (100 mM) was encapsulated in liposomes, and the release was monitored as a function of time (excitation, 480 nm; emission, 515 nm). Release from the nanovesicles was recorded for 60 min in 30 s intervals. The experiments were carried out in a 96-well plate (6 repeats for each measurement). Each well contained 20 μL of nanovesicles and 160 μL of HEPES buffer (pH 8) with added Ca²⁺ and Zn²⁺ ions (10 mM, osmolarity adjusted to 290 with NaCl). Recombinant human MMP-9 was prepared in our laboratory, as described previously.^{20,21} Contents released in response to added recombinant MMP-9 (2 μM) and GSH (50 μM) were monitored for 60 min. Release in human serum (10%) was also monitored for 60 min. After 60 min, Triton-X100 was added to each well to disrupt the nanovesicles, and emission intensity was measured. This intensity was considered to be for complete release of the encapsulated dye, and the percentage released for each experiment was calculated using the following formula:

$$\% \text{ release} = \left[\frac{\text{(emission intensity after 60 min)} - \text{initial intensity before treatment}}{\text{(emission intensity after Triton treatment)} - \text{initial intensity before treatment}} \right] \times 100$$

2.5. Cell Culture. Pancreatic cancer cell lines PANC-1 and MIAPaCa-2 were obtained from American Type Culture Collection (Manassas, VA). PANC-1 cells were cultured in RPMI media (without phenol red) that were supplemented with 2% antibiotics (penicillin, streptomycin) and 10% v/v fetal bovine serum. The MIAPaCa-2 cells were cultured in DMEM media that were supplemented with 2% horse serum and 2% antibiotics. All cell lines were grown at 37 °C in a humidified atmosphere containing 5% CO₂.

2.6. Alamar Blue Assay with a Monolayer Cell Culture. Cytotoxicity of the encapsulated gemcitabine was measured by treating the PANC-1 and MIAPaCa-2 cells with nanovesicles. The cells were incubated (1,000 per well) in a 96-well plate after trypsinizing the flask and making a cell suspension. RPMI media (100 μL) were added to each well. Cells were allowed to grow for one doubling time. The plate was divided into three groups: control, gemcitabine-treated, and gemcitabine-encapsulated nanovesicle treated. Six replicates were recorded for each sample. The control group did not receive any treatment. Phosphate buffer saline (PBS)-encapsulated liposomes were also employed as control for cell viability studies. Gemcitabine-

treated cells received 5 μM , 10 μM , and 20 μM gemcitabine, and nanovesicle-treated cells received an equivalent amount of encapsulated gemcitabine. The treatment was carried out for 3 days, and cell toxicity was recorded after 72 h with the Alamar Blue assay by following the supplier's (Life Technologies) protocol. Alamar Blue solution (10 μL) was added to all the wells and incubated for 2 h, and the absorbance was recorded at 585 nm for cytotoxicity calculation. Toxicity of PBS encapsulated nanovesicles was observed by incubating MIAPaCa-2 cells (1000 per well) in a 96-well plate with nanovesicles representing lipid concentrations ranging from 5 $\mu\text{g}/\text{mL}$ to 100 $\mu\text{g}/\text{mL}$. Alamar Blue assay was carried out to observe cell viability of MIAPaCa-2 cells after incubating for 72 h with the nanovesicles.

2.7. Estimation of Cell-Secreted MMP-9 Concentration. Conditioned media from confluent cultures of PANC-1 and MIAPaCa-2 cells were collected, and a concentration of secreted MMP-9 was estimated by using a commercially available MMP-9 ELISA kit (RayBio Tech). The manufacturer's instructions were followed to estimate the MMP-9 secreted by the cells.

2.8. Three-Dimensional Spheroid Cell Culture. Based on the ELISA results, the PANC-1 cell line was selected for the spheroid culture because it showed the highest levels of secreted MMP-9. In order to prepare the cell spheroids, agar molds, each having the capability to form 96 spheroids of uniform size, were created. To prepare the plates, a slightly modified protocol provided by Microtissues (http://www.microtissues.com/3dcellculture_protocols/Casting_Equilibrating_and_Seeding_the_3D_Petri_Dish.pdf) was used. The prepared plates were equilibrated with RPMI media for 1 h at 37 °C and placed in 6-well plates, and 2 mL of RPMI media was added to each well to provide nutrition for the cells seeded in the plates. Agar plates were then seeded with 75 μL of cell suspension containing 10,000 cells in each plate, which formed spheroids after 3 days of incubation at 37 °C. These spheroids were used for cell-viability and oxidative-stress studies.

2.9. Lactate Dehydrogenase (LDH) Assay. LDH was measured using a kit supplied by G-Biosciences (Cytoscan LDH Cytotoxicity assay). The manufacturer's instructions were followed to measure the LDH released in response to cytotoxicity caused by the release of gemcitabine from the nanovesicles. This assay was carried out using 1-day, 3-day, and 5-day old spheroids.

2.10. Alamar Blue Assay with 3-D Cell Culture. Plates containing 96 spheroids molds were prepared, and cells were allowed to grow for 5 days in order to form spheroids. These plates were divided into 3 groups on the basis of the treatment they received: control, drug treated, and drug-encapsulated nanovesicles. Each group contained 6 plates with 96 spheroids. The control group received the same nutrition media as the other groups. The drug-treated group received 10 μM gemcitabine, and the test group received drug-encapsulated nanovesicles (encapsulating 10 μM gemcitabine). Spheroids in all groups received the treatment for 72 h. Subsequently, all the media surrounding the micromold were removed. The spheroids were treated with TryPLE (Life Technologies) and were incubated for 1 h at 37 °C to ensure dissociation of all the cells in the spheroid. RPMI media (3 mL) were added to each plate and were triturated to remove all the cells from the plate. From the cell suspension obtained, 100 μL from each plate was seeded on a new clear-bottom, 96-well plate (repeated 6 times

for each well). Additional growth medium (100 μL) was added to all the wells receiving the cell suspension. The cells were allowed to grow for one doubling time, and the Alamar Blue assay was carried out per the manufacturer's protocol, as described before.

2.11. Confocal Fluorescence Microscopic Imaging. Carboxyfluorescein-encapsulated nanovesicles were used to visualize the release of contents in 7-day-old spheroids of PANC-1 cells. Nanovesicles devoid of lipopeptide LP were used as a control. The spheroids were treated in the plate with the control and sample nanovesicles by incubating for 4 h at 37 °C. The spheroids were then washed (3X) with culture media. Spheroid-holding plates were then centrifuged to dislodge spheroids in the media. These spheroids were then imaged using a Zeiss AxioObserver Z1, inverted microscope with an LSM700 laser-scanning head attachment and a 20X 0.4 LD Plan-Neofluar objective. The first and last appearance of the fluorescence in the sample-treated spheroids was set as the scanning range. The same comparison range was selected for the control spheroids. Images were processed with Zeiss AxioVision Rev. 4.8.1 image-analysis software (Carl Zeiss, Thornwood, NY).

2.12. *In Vivo* Imaging. For *in vivo* imaging, athymic, Nude-Foxn1 (female, 5–6 week old), nude mice were used. PANC-1 cells (3 million) were injected subcutaneously. A well-developed tumor was observed after 21 days, and this animal was used for the imaging studies. Carboxyfluorescein-encapsulated (50 mM) nanovesicles (60 μL) were injected via the tail vein. Images were recorded using a reflectance imaging system (Kodak *in vivo* system FX, Carestream Health, Inc., Rochester, NY). The whole-body fluorescence images were acquired using the FITC channel (excited at 480 nm and recorded at 680/720 nm) after 5 s of exposure. Images were recorded to monitor the release of carboxyfluorescein at the tumor site 6 and 24 h after injection. The images were further processed using Kodak Molecular Imaging software (version 4.0).

2.13. *In Vivo* Studies. *In vivo* studies were carried out using a xenograft model for athymic, Nude-Foxn1 (female, 5–6 week old), nude mice (IACUC-approved protocol number A13066). PANC-1 cells (3 million) were injected subcutaneously into the nude mice, and the cells were allowed to grow at the injected site for 15 days. After the tumors developed, mice were divided into the control, positive control, and test groups ($n = 3$ for each group). The control group received a phosphate buffer (pH 7.4, osmolarity 325 mOsm/kg), animals in the positive control group received gemcitabine (10 mg/kg/week) encapsulated in PEGylated liposomes devoid of LP, and the test group received a 10 mg/kg/week dose of gemcitabine-encapsulated in the designed MMP-9 responsive PEG cleavable nanovesicles. The treatment was administered for 4 weeks via tail-vein injection. The tumor size was recorded each week, and the tumor volume was calculated using the following formula: volume = (width)² × length/2. The mice's weights were recorded throughout the study, and the mice were closely monitored for any sign of toxicity.

3. RESULTS AND DISCUSSION

Coating the drug carriers with a layer of poly(ethylene glycol) or another hydrophilic polymer imparts the long-circulating property. However, efficient interactions between the drug carrier and tumor microenvironment require the removal of the protective PEG coating from the surface of the carrier at the

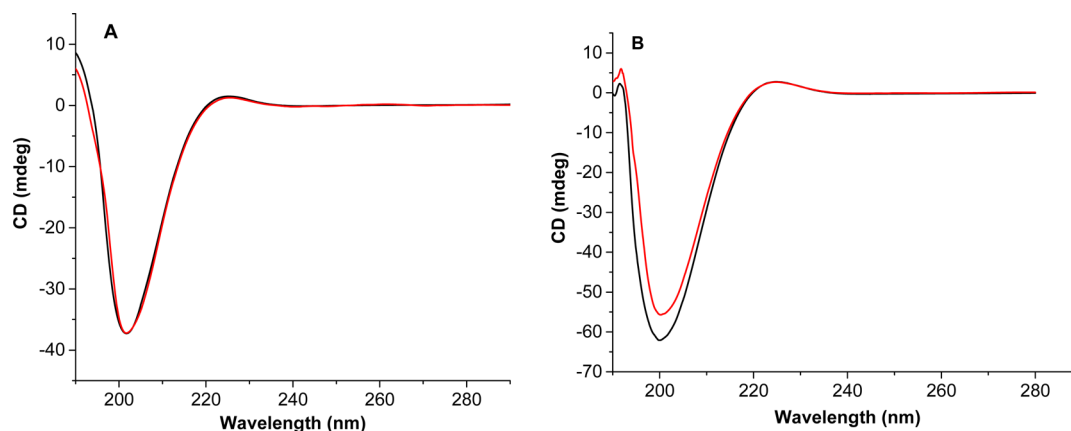


Figure 2. CD spectra of nanovesicles (black trace) and nanovesicles treated with 50 μM GSH (red trace) did not show any change in triple helicity (A), but treatment with MMP-9 (red trace) showed changes in the triple helicity of the nanovesicles (black trace) (B).

target site.²² In order to impart this feature to the nanovesicles, we synthesized a reduction-sensitive PEGylated lipid POPE-SS-PEG₅₀₀₀ (Scheme 1). The product was confirmed by NMR and MALDI mass spectral analysis (Supporting Information). We anticipated that the long PEG chains would protect the MMP-9 substrate lipopeptide LP from cleavage in the presence of low levels of MMP-9 (50–100 nM; found in the blood), and would provide long-circulating characteristics to the nanovesicles. Increased oxidative stress often results in elevated levels of glutathione (GSH) in tumor tissues.²³ The sulfhydryl group of reduced glutathione participates in the thiol exchange,²⁴ and this reaction is expected to reduce the disulfide bonds of the POPE-SS-PEG₅₀₀₀ lipid. We anticipate that the resultant exposure of the collagen mimetic, substrate lipopeptides to the elevated MMP-9 levels in the tumor extracellular matrix will initiate the hydrolysis of the lipopeptides, leading to destabilization of the nanovesicles.

The lipopeptide LP was designed to act as a substrate for the extracellular enzyme MMP-9.²⁵ We have previously demonstrated that LP can be successfully incorporated into the liposomal lipid bilayer and that the resultant vesicles undergo “uncorking” in the presence of elevated levels of catalytically active MMP-9, releasing the encapsulated contents.²⁰ We have also established that other cancer-associated MMPs, which do not hydrolyze triple helical peptides (e.g., MMP-7, MMP-10), are ineffective in releasing contents from these liposomes.^{21,25} However, MMP-2 and MMP-9 have similar substrate selectivity^{26,27} and are likely to hydrolyze LP. The collagen-mimetic, MMP-9, cleavable LP was synthesized by microwave-assisted, solid-phase peptide synthesis and was purified by reverse-phase HPLC (Supporting Information). The MMP-9 cleavage site for LP is located between the amino acids glycine and isoleucine.²⁵ The collagen-mimetic, triple-helical structural characteristic of purified LP was confirmed by CD spectroscopy, showing a positive peak at 220 nm and a negative peak at 198 nm (Supporting Information).²⁸

LP retained its triple helical structure when incorporated into nanovesicles composed of POPC (65%), POPE-SS-PEG (5%), and cholesteryl hemisuccinate (5%) (Figure 2A, black trace). We observed that the triple helicity of nanovesicle-incorporated LP was unchanged upon treatment with GSH (50 μM) for 1 h (Figure 2A, red trace). However, the triple helicity of LP was considerably reduced when incubated with 2 μM recombinant human MMP-9 for 60 min (Figure 2B, red trace).

The nanocarriers’ size is crucial for passive tumor targeting because the drug carriers accumulate at the target site by infiltration through the leaky vasculature.²⁹ The nanovesicles composed of POPC:LP:cholesteryl hemisuccinate:POPE-SS-PEG (60:30:5:5) were prepared with the thin film hydration method, followed by sonication and extrusion. The size of the prepared nanovesicles was assessed by dynamic light scattering at a 90° angle. The size of the vesicles immediately after passing through the size-exclusion column was observed to be 86 ± 18 nm with a polydispersity index (PDI) of 0.3. The size of these nanovesicles was retained for 24 h at room temperature. Treatment with MMP-9 (2 μM) and GSH (50 μM) for 24 h at room temperature increased the average size to 109 ± 20 nm with a PDI of 0.4 (Figure 3). Treatment with 50 μM GSH only

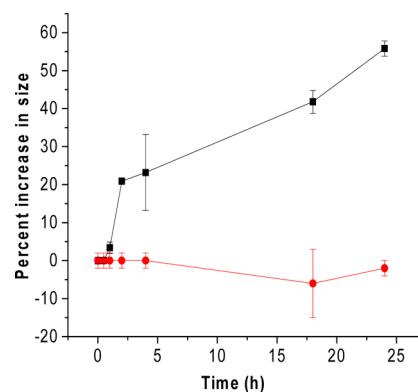


Figure 3. Nanovesicles treated with the MMP-9 (2 μM) and GSH (50 μM) showed an increased size with time (black squares, $n = 6$). The size of the untreated nanovesicles was not affected at room temperature (red circles, $n = 6$). The straight lines connecting the observed data points are shown in the plot.

led to a slight reduction in the sizes of the liposomes, possibly indicating the removal of the PEG groups (Supporting Information, Figure S4). Treatment with only MMP-9 (2 μM) resulted in a slight increase in the liposomal size (Supporting Information, Figure S4). A similar size increase was also observed when we repeated the experiment at 37 °C (Table S1, Supporting Information).

This change in size upon incubation with MMP-9 indicates that the hydrolysis of the triple-helical substrate peptides by MMP-9 leads to substantial structural changes in the vesicles,

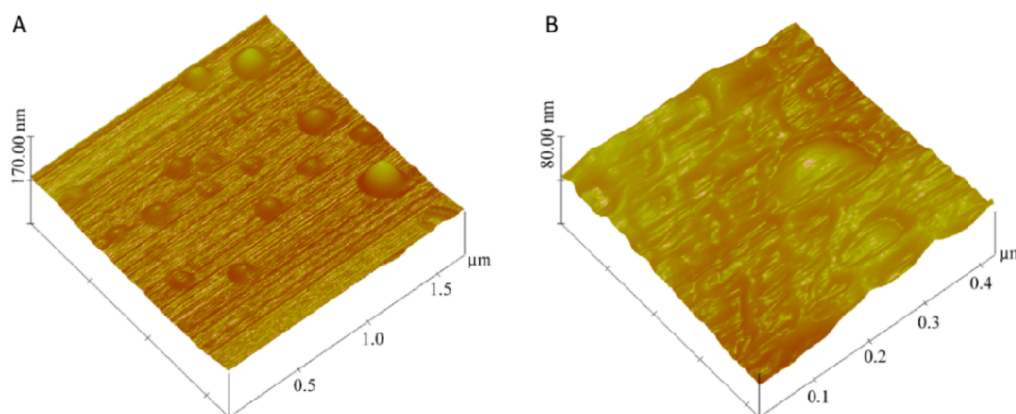


Figure 4. AFM images for the gemcitabine-encapsulated nanovesicles (A) before and (B) after 24 h of incubation with GSH (50 μM) and MMP-9 (2 μM).

resulting in the increased average diameter. The size change was also observed in the AFM imaging (Figure 4). The observed size of the nanovesicles increased after 24 h of treatment with MMP-9 and GSH at room temperature. Although the nanovesicles were expected to decrease in size as result of leakage through the bilayer, we observed an increase in the size of the nanovesicles treated with MMP-9 and GSH. After cleavage of the lipopeptides by MMP-9, nanovesicles undergo “uncorking” and release the encapsulated contents. This leads to the loss of integrity of the nanovesicles, possibly resulting in nonspecific aggregates of larger size. The liposomes which were not treated with MMP-9 showed less variation in size after 24 h.

For quantitative estimation of contents release from the nanocarrier we encapsulated carboxyfluorescein (100 mM) in the nanovesicles. The release was monitored as a function of time in the presence of added GSH (50 μM) and MMP-9 (2 μM) in pH 8.0 buffer. We have previously demonstrated that the release of liposomal contents requires catalytically active MMP-9.²¹ An increased release was observed with both the GSH and MMP-9 treatments. The nanovesicles exhibited about a 5% release over 1 h, in the presence of basal concentration of GSH observed in circulation (2- μM) (Figure 5, black squares). However, up to 22% of the encapsulated carboxyfluorescein

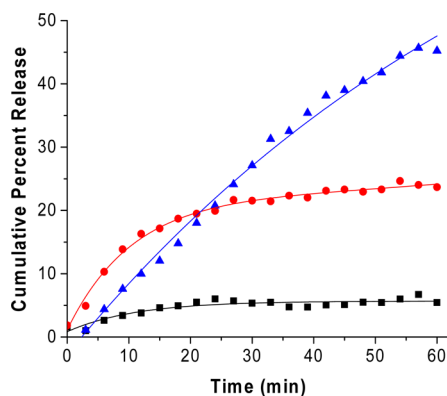


Figure 5. Cumulative release profiles from nanovesicles under circulatory conditions (2 μM GSH, black squares), in response to MMP-9 (2 μM , red circles), and with an extracellular tumor mimicking the environment composed of MMP-9 (2 μM) and GSH (50 μM , blue triangles). The traces represent the fitted curves using a single exponential-rate equation.

was released after 1 h of exposure to elevated levels of GSH found in tumor extracellular microenvironment (50 μM , Figure 5, red circles). To mimic the tumor’s extracellular matrix environment, the nanovesicles were exposed to elevated levels of MMP-9 (2 μM) and GSH (50 μM). In these conditions, we observed a 45% content release in 60 min (Figure 5, blue triangles). These release profiles can be fitted with a single exponential-rate equation with rate constants of $(12.5 \pm 0.6) \times 10^{-2} \text{ s}^{-1}$ for 2 μM MMP-9, $(11.1 \pm 2.2) \times 10^{-2} \text{ s}^{-1}$ for 2 μM GSH, and $(80.5 \pm 0.1) \times 10^{-2} \text{ s}^{-1}$ in the presence of 2 μM MMP-9 and 50 μM GSH. Note that the rate of content release was substantially higher in the presence of MMP-9 and GSH, as observed in the extracellular microenvironment of tumors. Based on literature reports^{30,31} and these observations, we conclude that the elevated levels of GSH are reductively removing the PEG groups from the POPE-S-S-PEG lipids. This facilitates the hydrolysis of LP by MMP-9, leading to the release of liposomal contents. We observed similar results when the release experiments were conducted at 37 $^{\circ}\text{C}$ (Supporting Information, Figure S4). As another control, we incubated the liposomes (without any added GSH and MMP-9) in buffers of different pH values (5.0, 6.0, 7.0, and 8.0) at room temperature, and at 37 $^{\circ}\text{C}$. We did not observe any significant release from the liposomes as a function of pH (release <5%).

A major challenge in designing an internal, stimulus-sensitive system is the stability of the carriers in circulation before reaching the target site. To test the stability of the prepared nanovesicles, we monitored the release of carboxyfluorescein in the presence of 10% human serum. The nanovesicles exhibited less than 5% release over a period of 1 h in 10% human serum (Supporting Information, Figure S2). The stability of nanovesicles in human serum was suggestive of the designed nanovesicles’ stability in circulatory conditions.

Having demonstrated the release of encapsulated dye, the *in vitro* and *in vivo* studies were carried out using gemcitabine-encapsulated nanovesicles. Gemcitabine was encapsulated in the nanovesicles with the pH gradient method, and entrapment efficiency was observed to be 50%. These nanovesicles were used to assess cytotoxicity for the pancreatic cancer cells (PANC-1 and MIAPaCa-2) in the monolayer cultures. The cells were treated with gemcitabine and gemcitabine-encapsulated nanovesicles for 72 h, and cell viability was measured with Alamar Blue dye. Both free and encapsulated gemcitabine showed similar toxicity for the PANC-1 (viability: 30–35%; Figure 6, blue bars) and MIAPaCa-2 cells (viability: 45–50%;

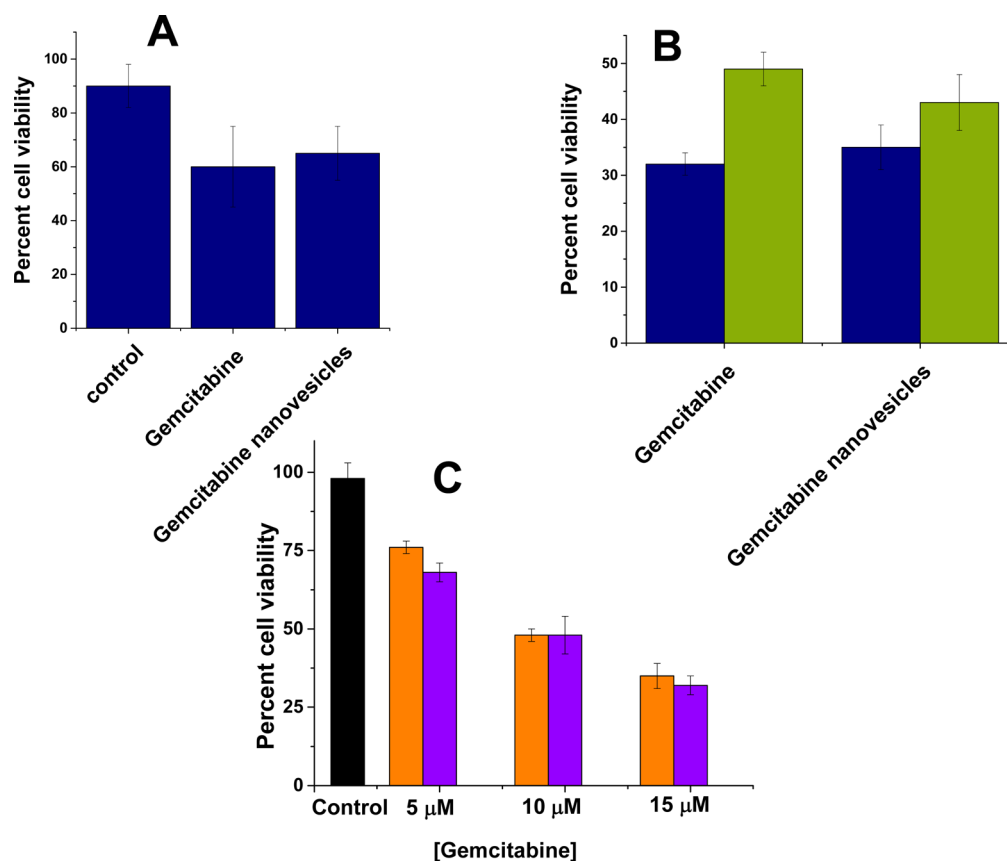


Figure 6. Cell viability observed in the monolayer (A) ($n = 6$) and spheroid (B) cultures ($n = 3$) of PANC-1 (blue) and MIAPaCa-2 cells (green) after 72 h treatment with gemcitabine ($10 \mu\text{M}$), gemcitabine nanovesicles (encapsulating $10 \mu\text{M}$ gemcitabine), and control nanovesicles encapsulating PBS (20 mM , pH 7.4). No significant difference was observed in cell viability of PANC-1 cells in 2-D and 3-D cultures when treated with gemcitabine or gemcitabine nanovesicles. Concentration dependent decrease in cell viability (C) was observed when the MIAPaCa-2 cells were treated with free gemcitabine (violet) or gemcitabine encapsulated nanovesicles (orange) for 72 h.

Figure 6, green bars). No apparent cytotoxicity was observed from nanovesicles themselves (Figure S5, Supporting Information). However, both free and liposome-encapsulated gemcitabine showed similar and dose-dependent toxicity (Figure 6C). We quantified the levels of secreted MMP-9 from these two cell lines by employing a commercially available ELISA kit. The results showed a higher concentration of MMP-9 in the conditioned media of PANC-1 cells ($126 \pm 23 \text{ pg/mL}$) compared to MIAPaCa-2 cells ($8 \pm 4 \text{ pg/mL}$). It is likely that the encapsulated gemcitabine was released from the nanovesicles by the MMP-9 secreted into the conditioned culture media. Hence, free and encapsulated gemcitabine demonstrated similar cytotoxicity, and the effect was more for the PANC-1 cells compared to the MIAPaCa-2 cells. To corroborate this hypothesis, we repeated the liposomal contents release experiments in the presence of the conditioned culture media of the brain endothelial cells bEnd-3. These cells do not express and secrete MMP-9 in the extracellular media.³² We observed minimal contents release from the liposomes in the presence of conditioned media from the bEnd-3 cells (Supporting Information, Table S2).

Subsequently, we cultured spheroids of uniform size by using micromolds in each well of a 6-well microplate. After seeding the PANC-1 cells, the spheroid growth was monitored for 7 days. With the increased size, the cells in the spheroid core undergo apoptosis due to a lack of oxygen and nutrients, mimicking the hypoxic conditions observed in tumor tissues.³³

This cell death in the spheroid core is reflected in increased LDH levels in the culture media.³⁴ We also observed a similar effect in the spheroid cultures of the PANC-1 cells (Figure 7).

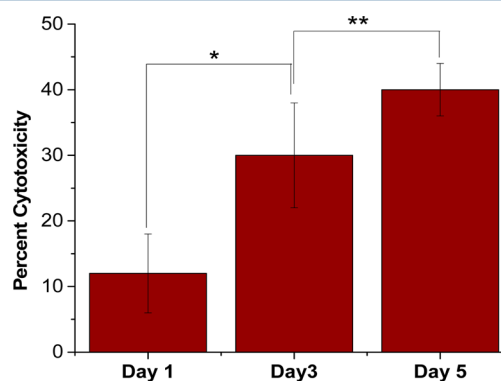


Figure 7. LDH released in response to cell death due to the hypoxic conditions in the spheroid core after 1, 3, and 5 days ($n = 6$, $*p < 0.001$, $**p < 0.05$).

We repeated the cytotoxicity assays with free and nanovesicle-encapsulated gemcitabine, employing the PANC-1 spheroids. We observed that the cell viability was similar in spheroids treated with the free and encapsulated drug (Figure 6B). We saw that the cytotoxicity for the encapsulated gemcitabine was

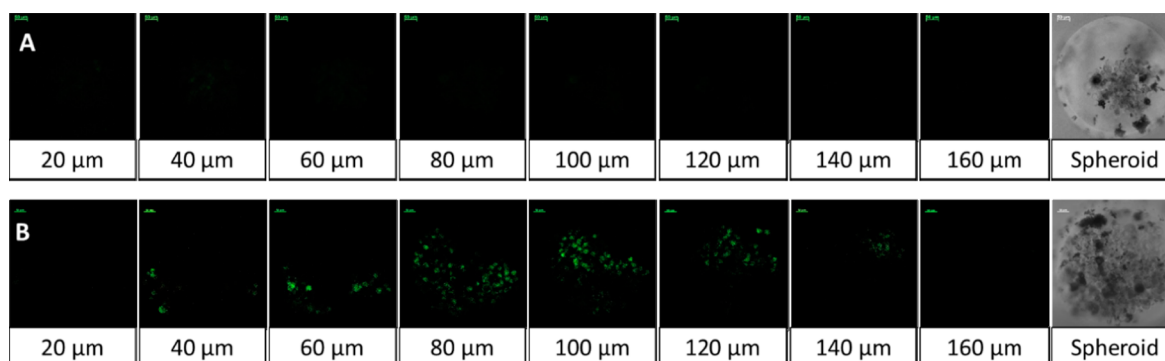


Figure 8. Uptake of released carboxyfluorescein by the spheroids of the PANC-1 cells. Spheroids treated with MMP-9-responsive nanovesicles showed an enhanced uptake of carboxyfluorescein released from the nanovesicle (B) as compared to nanovesicles that lacked the MMP-9 responsive lipopeptide (A).

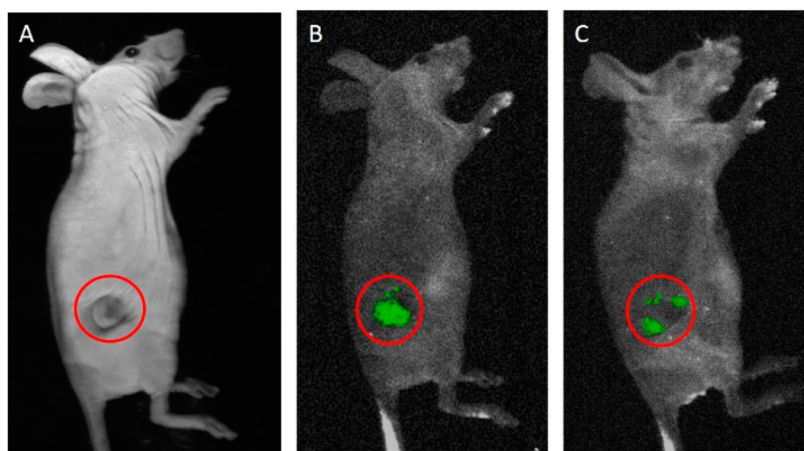


Figure 9. Carboxyfluorescein release from nanovesicles was observed after 6 h (B) and 24 h (C) of injection via the tail vein in nude mice. Panel A represents a white-light image, and the red circles indicate the tumor-bearing site.

less in spheroids compared to the two-dimensional cultures of the PANC-1 cells.

To ascertain that the encapsulated contents were released from the nanovesicles and internalized in the PANC-1 cell spheroids, we monitored the uptake with confocal fluorescence microscopy. For easier visualization, these experiments were conducted with carboxyfluorescein-encapsulated nanovesicles. We prepared analogous liposomes without incorporating the MMP-9 substrate peptide LP and used these nanovesicles as the control. Since our objective was to demonstrate that the encapsulated dye is released by the tumor spheroids, we did not add any GSH to the culture media. We observed that the control nanovesicles failed to release the contents, and no significant dye internalization was detected (Figure 8A). However, the nanovesicles with LP efficiently released the encapsulated carboxyfluorescein and the dye was internalized in the spheroids (Figure 8B).

The nanovesicles were observed to be stable in 10% human serum, suggesting stability in circulation before reaching the tumor site (Figure S2, Supporting Information). Live-animal imaging after 6 and 24 h of tail-vein administration of carboxyfluorescein-encapsulated nanovesicles confirmed the stability and the effective release capability at the tumor site (Figure 9).

Subsequently, we proceeded to demonstrate the effectiveness of the proposed delivery strategy by employing a xenograft mouse model of human pancreatic cancer. For these studies, we

used 9 athymic, female, Nude-Foxn1nu mice (5–6 weeks old). The mice were divided into three groups (control, positive control, and test) and were injected with 3 million PANC-1 cells subcutaneously. Tumors developed in the animals, 15 days after subcutaneous injections. The objective of this study was to demonstrate the release of encapsulated gemcitabine from the PEGylated nanovesicles in response to elevated levels of proteolytic enzyme MMP-9 in tumor extracellular matrix. Studies on the *in vivo* toxicity of gemcitabine and benefit of using gemcitabine encapsulated liposomes are already reported.^{35,36} Hence, for our studies, the control group received weekly injections (via the tail vein) of buffer. The animals in positive control and test groups received injections of gemcitabine-encapsulated nanovesicles (without and with LP, respectively; dose: 10 mg/kg/week) for 4 weeks. The animals from both groups showed lesser tumor growth as compared to the control (Figure 10). However, we observed that the animals receiving gemcitabine encapsulated in PEGylated MMP-9 responsive nanovesicles showed more pronounced reduction in tumor growth (Figure 10, blue triangles) as compared to animals receiving gemcitabine encapsulated in PEGylated liposomes without LP (Figure 10, red circles). Weight for all the animals receiving gemcitabine nanovesicles did not decrease during and after the treatment, indicating the lack of toxicity for the nanovesicle formulations (Supporting Information). After 4 weeks of treatment, we observed that the increased tumor

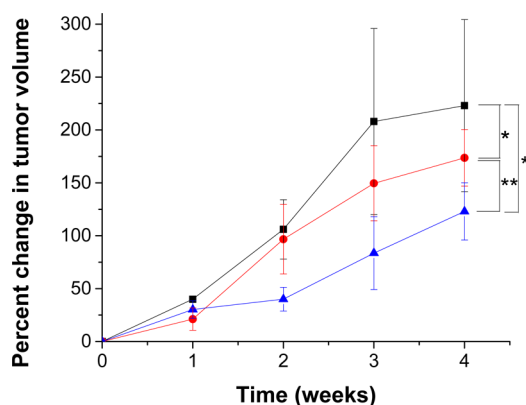


Figure 10. Percentage increase in tumor volume for the test group (blue triangles, $n = 3$) was lower in LP-incorporated nanovesicle-treated mice as compared to the control (black squares, $n = 3$) and positive control treated mice (red circles, $n = 3$) (* $p < 0.05$, ** $p < 0.05$).

volumes for the treated mice were substantially less compared to the control group (Figure 10).

4. CONCLUSIONS

We have successfully demonstrated that the elevated levels of MMP-9 and GSH in the extracellular matrix of tumor tissues can be used to trigger contents release from suitably constructed nanovesicles. These liposomes incorporate disulfide-linked PEG groups on the surface. At the tumor site, elevated levels of glutathione reductively remove the PEG groups, exposing the MMP-9 substrate peptide toward enzymatic hydrolysis. The resultant destabilization of the lipid bilayer leads to rapid release of encapsulated contents. We have successfully encapsulated the anticancer drug gemcitabine and demonstrated that the cytotoxicity of the released drug to pancreatic cancer cells (in monolayer and spheroid cultures) is comparable to that for the nonencapsulated drug. Internalization studies carried out using pancreatic cancer cell spheroids showed that the incorporated MMP-9-responsive lipopeptide triggers the drug release in the tumor's extracellular matrix. *In vivo* imaging studies with the designed, long-circulating nanovesicles exhibited circulatory stability. *In vivo* studies also confirmed the release of encapsulated gemcitabine in the tumor microenvironment, showing a reduction in tumor growth rate in nude mice. We observed better control over tumor growth with the MMP-9 responsive nanovesicles compared to the PEGylated vesicles without the MMP-9 substrate lipopeptide.

■ ASSOCIATED CONTENT

Supporting Information

Synthesis and characterization details for the POPE-S-S-PEG lipid and the lipopeptide, calculation of gemcitabine encapsulation efficiency, release and size analysis studies at 37 °C, and cellular toxicity of the nanovesicles. This material is available free of charge via the Internet at <http://pubs.acs.org>.

■ AUTHOR INFORMATION

Corresponding Author

*E-mail: Sanku.Mallik@ndsu.edu. Phone: (001)-7012317888.

Notes

The authors declare no competing financial interest.

■ ACKNOWLEDGMENTS

This research was supported by NIH Grant 1R01 CA 113746 as well as NSF Grants DMR 1005011 and DMR 1306154 to S.M. and D.K.S.

■ REFERENCES

- (1) Fleige, E.; Quadir, M. A.; Haag, R. Stimuli-responsive polymeric nanocarriers for the controlled transport of active compounds: Concepts and applications. *Adv. Drug Delivery Rev.* **2012**, *64* (9), 866–884.
- (2) Ganta, S.; Devalapally, H.; Shahiwala, A.; Amiji, M. A review of stimuli-responsive nanocarriers for drug and gene delivery. *J. Controlled Release* **2008**, *126* (3), 187–204.
- (3) Radhakrishnan, K.; Tripathy, J.; Raichur, A. M. Dual enzyme responsive microcapsules simulating an “OR” logic gate for biologically triggered drug delivery applications. *Chem. Commun.* **2013**, *49* (47), 5390–2.
- (4) de la Rica, R.; Aili, D.; Stevens, M. M. Enzyme-responsive nanoparticles for drug release and diagnostics. *Adv. Drug Delivery Rev.* **2012**, *64* (11), 967–978.
- (5) Coleman, J. D.; Thompson, J. T.; Smith, R. W., 3rd; Prokopczyk, B.; Vanden, H. J. P. Role of Peroxisome Proliferator-Activated Receptor β/δ and B-Cell Lymphoma-6 in Regulation of Genes Involved in Metastasis and Migration in Pancreatic Cancer Cells. *PPAR Res.* **2013**, *2013*, 121956.
- (6) Tauro, J. R.; Gemeinhart, R. A. Matrix metalloprotease triggered delivery of cancer chemotherapeutics from hydrogel matrices. *Bioconjugate Chem.* **2005**, *16* (5), 1133–9.
- (7) Molineux, G. PEGylation: engineering improved pharmaceuticals for enhanced therapy. *Cancer Treat Rev.* **2002**, *28* (Suppl. A), 13–16.
- (8) Moribe, K.; Maruyama, K. Reviews on PEG coated liposomal drug carriers. *Drug Delivery Syst.* **2001**, *16* (3), 165–171.
- (9) Liu, D.-L.; Chang, X.; Dong, C.-M. Reduction- and thermo-sensitive star polypeptide micelles and hydrogels for on-demand drug delivery. *Chem. Commun.* **2013**, *49* (12), 1229–1231.
- (10) Li, J.; Ge, Z.; Liu, S. PEG-sheddable polyplex micelles as smart gene carriers based on MMP-cleavable peptide-linked block copolymers. *Chem. Commun.* **2013**, *49*, 6974–6976.
- (11) Määttä, M.; Soini, Y.; Liakka, A.; Autio-Harminen, H. Differential expression of matrix metalloproteinase (MMP)-2, MMP-9, and membrane type 1-MMP in hepatocellular and pancreatic adenocarcinoma: implications for tumor progression and clinical prognosis. *Clin. Cancer Res.* **2000**, *6* (7), 2726–2734.
- (12) Yingyuad, P.; Mevel, M.; Prata, C.; Furegati, S.; Kontogiorgis, C.; Thanou, M.; Miller, A. D. Enzyme-Triggered PEGylated pDNA-Nanoparticles for Controlled Release of pDNA in Tumors. *Bioconjugate Chem.* **2013**, *24* (3), 343–362.
- (13) Koo, A. N.; Lee, H. J.; Kim, S. E.; Chang, J. H.; Park, C.; Kim, C.; Park, J. H.; Lee, S. C. Disulfide-cross-linked PEG-poly(amino acid)s copolymer micelles for glutathione-mediated intracellular drug delivery. *Chem. Commun.* **2008**, No. 48, 6570–6572.
- (14) Ren, T.-B.; Xia, W.-J.; Dong, H.-Q.; Li, Y.-Y. Sheddable micelles based on disulfide-linked hybrid PEG-polypeptide copolymer for intracellular drug delivery. *Polymer* **2011**, *52* (16), 3580–3586.
- (15) Zhang, A.; Zhang, Z.; Shi, F.; Ding, J.; Xiao, C.; Zhuang, X.; He, C.; Chen, L.; Chen, X. Disulfide crosslinked PEGylated starch micelles as efficient intracellular drug delivery platforms. *Soft Matter* **2013**, *9* (7), 2224–2233.
- (16) Abbott, A. Cell culture: biology's new dimension. *Nature* **2003**, *424* (6951), 870–872.
- (17) Phung, Y. T.; Barbone, D.; Broaddus, V. C.; Ho, M. Rapid generation of in vitro multicellular spheroids for the study of monoclonal antibody therapy. *J. Cancer* **2011**, *2*, 507.
- (18) Longati, P.; Jia, X.; Eimer, J.; Wagman, A.; Witt, M.-R.; Rehnmark, S.; Verbeke, C.; Toftgård, R.; Löhr, M.; Heuchel, R. L. 3D pancreatic carcinoma spheroids induce a matrix-rich, chemoresistant phenotype offering a better model for drug testing. *BMC Cancer* **2013**, *13* (1), 1–13.

(19) Celano, M.; Calvagno, M. G.; Bulotta, S.; Paolino, D.; Arturi, F.; Rotiroti, D.; Filetti, S.; Fresta, M.; Russo, D. Cytotoxic effects of gemcitabine-loaded liposomes in human anaplastic thyroid carcinoma cells. *BMC Cancer* **2004**, *4* (1), 63.

(20) Sarkar, N.; Banerjee, J.; Hanson, A. J.; Elegbede, A. I.; Rosendahl, T.; Krueger, A. B.; Banerjee, A. L.; Tobwala, S.; Wang, R.; Lu, X.; Mallik, S.; Srivastava, D. K. Matrix metalloproteinase-assisted triggered release of liposomal contents. *Bioconjugate Chem.* **2008**, *19* (1), 57–64.

(21) Elegbede, A. I.; Banerjee, J.; Hanson, A. J.; Tobwala, S.; Ganguli, B.; Wang, R.; Lu, X.; Srivastava, D. K.; Mallik, S. Mechanistic studies of the triggered release of liposomal contents by matrix metalloproteinase-9. *J. Am. Chem. Soc.* **2008**, *130* (32), 10633–10642.

(22) Li, S.-D.; Huang, L. Stealth nanoparticles: high density but sheddable PEG is a key for tumor targeting. *J. Controlled Release* **2010**, *145* (3), 178.

(23) Estrela, J. M.; Ortega, A.; Obrador, E. Glutathione in cancer biology and therapy. *Crit. Rev. Clin. Lab. Sci.* **2006**, *43* (2), 143–181.

(24) Pompella, A.; Visvikis, A.; Paolicchi, A.; Tata, V. D.; Casini, A. F. The changing faces of glutathione, a cellular protagonist. *Biochem. Pharmacol.* **2003**, *66* (8), 1499–1503.

(25) Banerjee, J.; Hanson, A. J.; Gadam, B.; Elegbede, A. I.; Tobwala, S.; Ganguly, B.; Wagh, A. V.; Muhonen, W. W.; Law, B.; Shabb, J. B.; Srivastava, D. K.; Mallik, S. Release of liposomal contents by cell-secreted matrix metalloproteinase-9. *Bioconjugate Chem.* **2009**, *20* (7), 1332–1339.

(26) Akers, W. J.; Xu, B.; Lee, H.; Sudlow, G. P.; Fields, G. B.; Achilefu, S.; Edwards, W. B. Detection of MMP-2 and MMP-9 activity in vivo with a triple-helical peptide optical probe. *Bioconjugate Chem.* **2012**, *23* (3), 656–663.

(27) Knapinska, A.; Fields, G. B. Chemical biology for understanding matrix metalloproteinase function. *ChemBioChem* **2012**, *13* (14), 2002–2020.

(28) Nahire, R.; Paul, S.; Scott, M. D.; Singh, R. K.; Muhonen, W. W.; Shabb, J.; Gange, K. N.; Srivastava, D. K.; Sarkar, K.; Mallik, S. Ultrasound enhanced matrix metalloproteinase-9 triggered release of contents from echogenic liposomes. *Mol. Pharmaceutics* **2012**, *9* (9), 2554–2564.

(29) Choi, M.-R.; Stanton-Maxey, K. J.; Stanley, J. K.; Levin, C. S.; Bardhan, R.; Akin, D.; Badve, S.; Sturgis, J.; Robinson, J. P.; Bashir, R. A cellular Trojan Horse for delivery of therapeutic nanoparticles into tumors. *Nano Lett.* **2007**, *7* (12), 3759–3765.

(30) Han, L. F.; Chen, Q. B.; Hu, Z. T.; Piao, J. G.; Hong, C. Y.; Yan, J. J.; You, Y. Z. Stimuli-triggered growth and removal of a bioreducible nanoshell on nanoparticles. *Macromol. Rapid Commun.* **2014**, *35* (6), 649–654.

(31) Cai, X.; Dong, C.; Dong, H.; Wang, G.; Pauletti, G. M.; Pan, X.; Wen, H.; Mehl, I.; Li, Y.; Shi, D. Effective gene delivery using stimulus-responsive cationer designed with redox-sensitive disulfide and acid-labile imine linkers. *Biomacromolecules* **2012**, *13* (4), 1024–1034.

(32) Chen, F.; Ohashi, N.; Li, W.; Eckman, C.; Nguyen, J. H. Disruptions of occludin and claudin-5 in brain endothelial cells in vitro and in brains of mice with acute liver failure. *Hepatology* **2009**, *50* (6), 1914–1923.

(33) Sutherland, R. M. Cell and environment interactions in tumor microregions: the multicell spheroid model. *Science* **1988**, *240* (4849), 177–184.

(34) Sasaki, T.; Ohno, T. Cytotoxicity tests on eye drop preparations by LDH release assay in human cultured cell lines. *Toxicol. In Vitro* **1994**, *8* (5), 1113–1119.

(35) Cosco, D.; Bulotta, A.; Ventura, M.; Celia, C.; Calimeri, T.; Perri, G.; Paolino, D.; Costa, N.; Neri, P.; Tagliaferri, P.; Tassone, P.; Fresta, M. In vivo activity of gemcitabine-loaded PEGylated small unilamellar liposomes against pancreatic cancer. *Cancer Chemother. Pharmacol.* **2009**, *64* (5), 1009–1020.

(36) Brusa, P.; Immordino, M. L.; Rocco, F.; Cattel, L. Antitumor activity and pharmacokinetics of liposomes containing lipophilic gemcitabine prodrugs. *Anticancer Res.* **2007**, *27* (1A), 195–199.